Fabrication of Cell Chip for Detection of Cell Cycle Progression Based on Electrochemical Method

ARTICLE *in* ANALYTICAL CHEMISTRY · FEBRUARY 2011

Impact Factor: 5.64 · DOI: 10.1021/ac102895b · Source: PubMed

4 AUTHORS, INCLUDING:

Tae-Hyung Kim
Chung-Ang University
34 PUBLICATIONS **313** CITATIONS
SEE PROFILE

Jeung Hee An
Konkuk University
42 PUBLICATIONS **262** CITATIONS
SEE PROFILE

analytical chemistry

ARTICLE

pubs.acs.org/ac

Fabrication of Cell Chip for Detection of Cell Cycle Progression Based on Electrochemical Method

Md. Abdul Kafi,[†] Tae-Hyung Kim,[‡] Jeung Hee An,[‡] and Jeong-Woo Choi*[,†,‡]

[†]Interdisciplinary Program of Integrated Biotechnology and [‡]Department of Chemical & Biomolecular Engineering, Sogang University, Shinsu-Dong, Mapo-Gu, Seoul 121-742, Republic of Korea

Supporting Information

ABSTRACT: A new strategy for on-site monitoring of cell cycle progression was proposed using cell chip technology. Cell synchronization has been utilized in intensive cellular research due to the fact that cells in different phases of the cell cycle exhibit different behaviors even when exposed to the same concentrations of drugs or toxicants. However, confirmation of cell cycle arrest in research is usually dependent on fluorescence-assisted cell sorting (FACS), which is laborious, time-consuming, and expensive. In this study, we employed a cell-chip-based electrochemical method to detect the cell-cycle-dependent electrochemical properties of cells. Electron transfer at the cell−electrode interface played a key role in our strategy and accurately reflected the redox activity of the cells in different phases. Rat pheochromocytoma cells were synchronized with thymidine and nocodazole, and well-defined current peaks from cells in the G1/S- and G2/M-phases were significantly different as determined by differential pulse voltammetry. FACS assay and Western blot analysis were used to validate the electrochemical findings. Hence, our cell-chip-based electrochemical method can be a useful tool in determining cell cycle progression easily and economically.

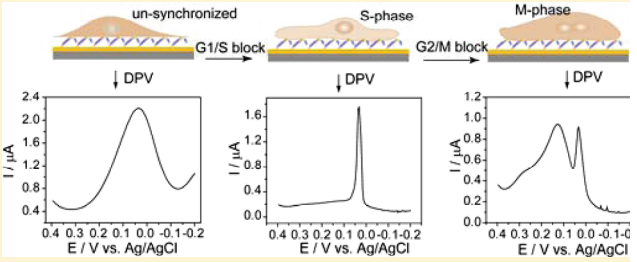

The cell cycle is a ubiquitous spontaneous process involving the growth and proliferation of cells that is essential to organismal development. Cells tend to show cycle-dependent characteristics, which are defined by a sequence of events in which several specific nuclear changes occur.[1] Many complex stages comprise the cell cycle; however, on the basis of morphological changes, the cell cycle can be broadly subdivided into interphase and mitotic (M)-phase stages.[2] The M-phase includes several subphases, including the prophase, metaphase, anaphase, and telophase.[2] Similarly, the interphase encompasses the G1-, S-, and G2-phases, where the G1- and G2-phases represent "pauses" in the cell cycle that occur between DNA synthesis and mitosis.[3] The G1-phase is the first pause in which cells prepare for DNA synthesis. In the S-phase, cells synthesize DNA and thus have aneuploidic DNA content between 2N and 4N.[4] Conversely, the G2-phase is the second pause of the cell cycle in which the cell prepares for mitosis (M-phase). On the basis of the cell cycle stages, checkpoints for DNA damage are classified into three stages: G1/S (G1), intra-S-phase, and G2/M checkpoints.[5]

Artificial regulation of the cell cycle is very important in cell-based research since cells in different stages react differently even when maintained under the same environmental conditions. Since cells are unsynchronized in their natural state, nontoxic specific materials are essential for cell synchronization. Thymidine and nocodazole are potential regulators of cell cycle arrest[6−10] and have been used to identify and separate cells in different stages by fluorescence-activated cell sorting (FACS) assay,[11−13] imaging using molecular probes,[9,10] and Western blot analysis using cell-cycle-dependent proteins.[14] However, all of these methods inevitably require conjugation of fluorescent probes for cell sorting, which is time-consuming, laborious, and expensive. For this reason, electrochemical impedance sensing was recently introduced as a new tool for monitoring cell cycle progression.[22] This impedance-based technique was proved as a useful tool for the detection of the effects of thymidine on cell cycle progression simply and easily by eliminating the external dyes or devices essential for conventional methods. However, cells in different cell cycle stages could not be clearly differentiated due to the limitation of the technique, which only detects the impedance between the cell and electrode surface. Therefore, a simple and rapid method with high sensitivity is still of great interest for the confirmation of cell cycle arrest.

We recently introduced cell chip technology capable of effectively measuring changes in cell viability upon exposure to different kinds of environmental toxins[15,16] or anticancer drugs[17,18] on the basis of simple and rapid electrochemical techniques. These electrical or electrochemical methods also have been incorporated into cell-based sensor arrays[19] as well as electrical

Received: November 4, 2010
Accepted: January 13, 2011
Published: February 16, 2011

dx.doi.org/10.1021/ac102895b | *Anal. Chem.* 2011, 83, 2104–2111

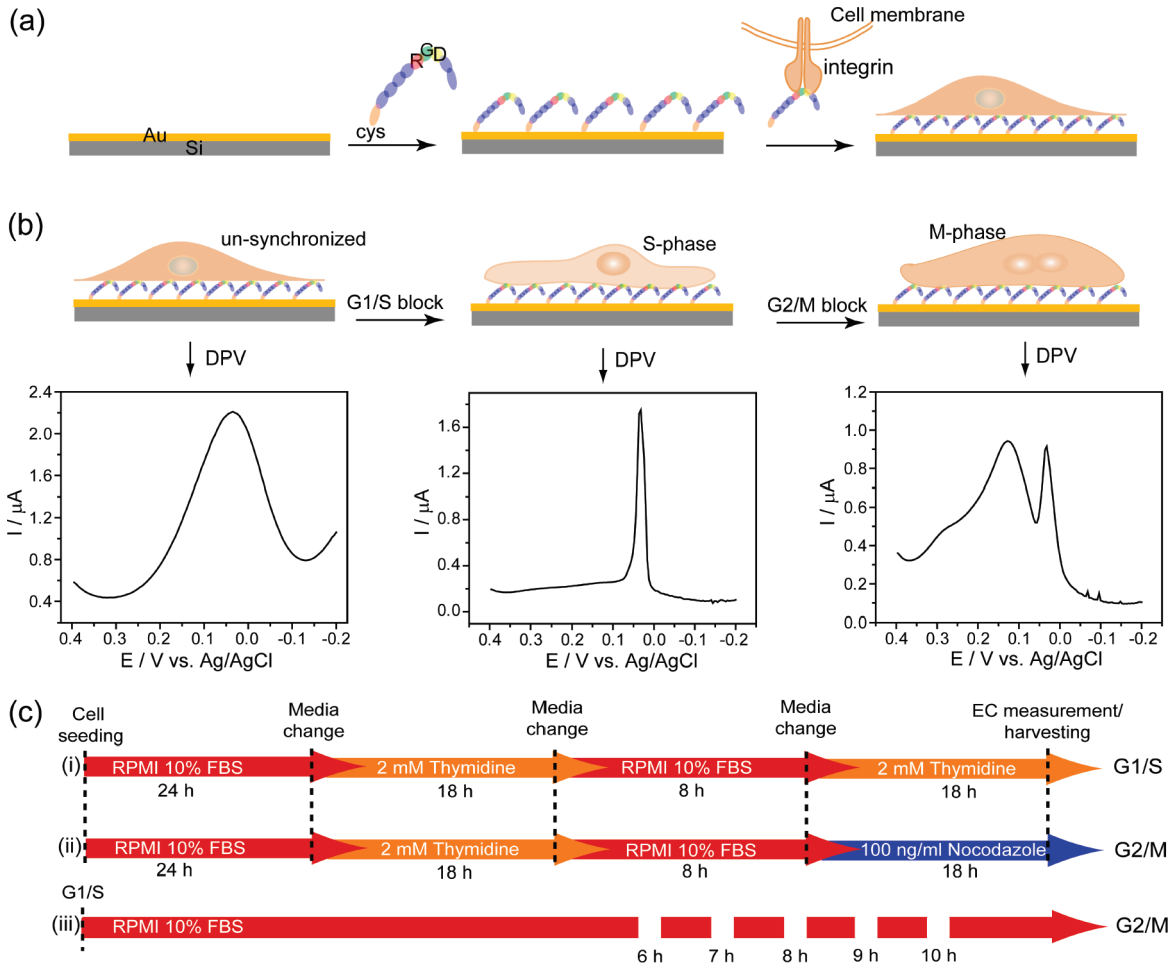

Figure 1. Schematic of the experimental setup: (a) fabrication of the RGD-MAP-C-based cell chip used throughout the experiments, (b) synchronized G1/S-phase (middle), G2/M-phase (right), and unsynchronized (left) cells with their respective DPV signals (arrows indicate the respective signals), and (c) time course of cell treatment for synchronization in the G1/S-phase (i) and G2/M-phase (ii) and gradual progression of G1/S cells toward the G2/M-phase following time-dependent release from the G1/S block (iii).

sensing devices for the detection of signal-frequency patterns produced by cells in growth media.[20,21] On the basis of previous reports, we found that the redox phenomenon at the cell−electrode interface[15] determine the electrophysiological characteristics of target cells, which vary depending on the cell line.[15−18] Since different kinds of cell lines were found to give different electrochemical signals, we hypothesized that the same cell line but in a different cell cycle stage will give different electrochemical signals, which can be used for determining cell cycle arrest as a potential label-free technology.

In the present study, PC12 cells were used to determine the potential of our method in confirming cell cycle arrest. Cells on the electrode surface were synchronized in the G1/S- and G2/M-phases using thymidine and nocodazole[23] to measure the phase-specific electrochemical signals. These electrochemical signals were further compared with the results from FACS and Western blot analysis.

EXPERIMENTAL SECTION

Chemicals. Thymidine and nocodazole were purchased from Sigma and used without further purification. Oligopeptide RGD-MAP-C was obtained from Peptron (Daejeon, South Korea). RPMI 1640 medium was purchased from Fresh Media (Daegu, South Korea). Fetal bovine serum (FBS), antibiotics (penicillin−streptomycin, 10 000 U/mL penicillin sodium and 10 000 μg/mL streptomycin sulfate in 0.83% saline), and trypsin (0.05% trypsin, 0.53 mM EDTA−4Na) were obtained from Gibco (Invitrogen, Grand Island, NY). Phosphate-buffered saline (PBS) (pH 7.4, 10 mM) was purchased from Sigma-Aldrich (St. Louis, MO). All other chemicals were of analytical grade. All solutions were prepared with doubly distilled water, which was purified using a Milli-Q purification system (Barnstead) to a specific resistance of >18 MΩ cm.

Preparation of the Working Electrode. A silicon-based gold electrode was first cleaned with freshly prepared piranha solution (1:3 mixture of 30% H_2O_2 and concentrated H_2SO_4) for 5 min and then rinsed thoroughly with doubly distilled water. The electrode was then carefully polished by sonication in absolute alcohol and doubly distilled water for 5 min. Finally, the electrode was electrochemically cleaned in 0.5 M H_2SO_4 until a stable cyclic voltammogram was obtained and then dried with purified nitrogen. After the pretreatment, a well-ordered oligopeptide (RGD-MAP-C) was fabricated on the freshly cleaned gold electrode as reported in our previous work.[15] For the electrochemical measurements, a 2 cm × 1 cm × 0.5 cm (width × length × height) cell chip chamber was fabricated

dx.doi.org/10.1021/ac102895b |*Anal. Chem.* 2011, 83, 2104–2111

by fixing a plastic chamber (Lab-Tek(R), Thermo Fisher Scientific, Waltham, MA) to the Au working electrode using poly(dimethylsiloxane), which produced an exposure area of approximately 2 cm × 1 cm. Afterward, rat pheochromocytoma (PC12) cells were seeded on the electrode at a density of 2 × 10^5 cells/chip and then immobilized via RGD−integrin interaction for 24 h in a standard cell culture environment.

Preparation of the G1/S and G2/M Blocks. The cell-immobilized electrode was treated with 2 mM thymidine in culture medium (RPMI 1640) for 18 h, followed by an 8 h release (replaced by fresh medium), and then again with 2 mM thymidine for another 18 h to block cells in the G1/S-phase (Figure 1c,i). Similarly, another cell-immobilized electrode was treated initially with 2 mM thymidine as mentioned before for 18 h, followed by a 4 h release (replaced by fresh medium), and then with 100 ng/mL nocodazole for another 10 h to block cells in the G2/M-phase (Figure 1c,ii). Thus, the working electrodes were prepared for electrochemical signal analysis of the cells in different phases of the cell cycle. Furthermore, for the time-dependent progression of the G1/S-phase toward the G2/M-phase, G1/S-blocked cells were released in fresh medium containing 10% FBS for several hours as shown in Figure 1c,iii. Considering the potential toxicity of thymidine and nocodazole, the whole experiments were conducted under a biosafety environment.

Electrochemical Measurements. Electrochemical measurements were carried out with a CHI660C potentiostat (CH Instruments). The commonly used three-electrode configuration was employed for the electrochemical measurements, whereas standard silver (Ag/AgCl) served as the reference electrode and a platinum wire as the counter electrode (Supporting Information, Figure S1). Prior to the electrochemical measurements, a gold electrode with G1/S- and G2/M-phase cells was washed twice with 10 mM PBS buffer (pH 7.4). Finally, electrochemical measurements were performed using 2 mL of the same PBS solution as the electrolyte. Before the measurements, the buffer solution was first thoroughly bubbled with high-purity nitrogen for 30 min. Then a stream of nitrogen was blown gently across the surface of the solution to prevent exposure to aerobic oxygen throughout the experiment. To minimize the scan effect, several repeated scannings were performed and the differential pulse voltammetry (DPV) signal from the third scan was selected for all the measurements throughout the study (Supporting Information, Figure S2). Moreover, all measurements were performed independently at least three times, and error bars are shown in the figures.

FACS Analysis. Thymidine- and nocodazole-treated synchronized cells were collected and fixed by resuspension in 0.5 mL of 70% ethanol for 30 min, followed by centrifugation at 1000 rpm for 10 min and washing in ice-cold PBS. The resulting cell pellets were then resuspended in 0.5 mL of PBS containing 50 μg/mL propidiumiodide (Sigma-Aldrich) and 100 μg/mL RNase (Invitrogen, Carlsbad, CA), followed by incubation at 37 °C for 30 min. Cell cycle distribution was examined by measuring the DNA content using a flow cytometer (FACS Caribur flow cytometer, Becton Dickinson, San Jose, CA) as described previously.[24] A minimum of 10^4 cells per data point were subjected to examination. The regions marked M1, M2, and M3 represent the G1, S, and G2/M-phases of the cell cycle, respectively.

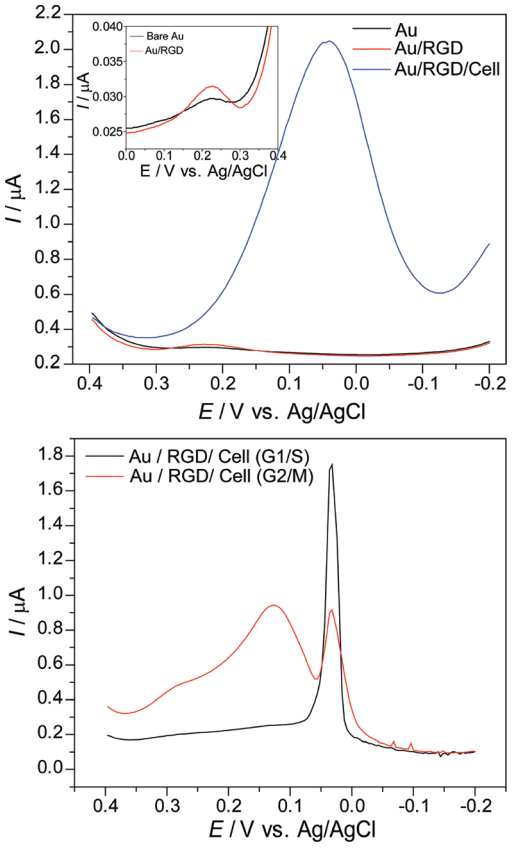

Figure 2. Electrochemical characterization of the fabricated cell-based chip: (a, top) DPV signals measured from bare Au, peptide-fabricated Au, and a cell-immobilized peptide-fabricated electrode (the inset shows the signal differences between bare Au and Au/RGD), (b, bottom) DPV signals measured from the chip synchronized in the G1/S-phase and G2/M-phase. DPV was measured using PBS (0.01 M, pH 7.4) as an electrolyte at a scan rate of 100 mV s^{-1}. The pulse amplitude and pulse width were 50 mV and 50 ms, respectively. The whole experiment was conducted at a temperature of 27 ± 1 °C using Pt and Ag/AgCl as the counter and reference electrodes, respectively.

Protein Assay. The synchronized PC12 cell pellet was solubilized for 15 min at 4 °C in lysis buffer. Lysates were centrifuged at 13000*g* for 30 min at 4 °C to remove insoluble material. The supernatant was then collected, and the protein concentration was determined using BCA protein assay reagent (Pierce Chemicals). For Western blot analysis, samples (25 μg each) were separated by electrophoresis on sodium dodecyl sulfate−polyacrylamide gels (12% for actin and cycline B1, 16% for phosphohistone-H^3 (p-HH^3)) and then transferred onto polyvinylidene difluoride membranes (Bio-Rad). The membranes were probed with anti-p-HH^3 (1:2000; Cell Signaling), anticycline B1 (1:2000; Abchem), and anti-β-actin (A-5441, 1:10000). The membranes were incubated with the respective antibodies at 4 °C overnight. After three washes with PBS containing 0.015% (v/v) Tween-20 for 10 min each, the membranes were incubated with secondary antibody (antimouse immunoglobulin G−horseradish peroxidase (IgG−HRP) for actin, antirabbit IgG−HRP for cycline B1 and p-HH^3) for 1 h at room temperature. The membranes were washed again three times and then developed using enhanced chemiluminescence (Amersham Biosciences, Uppsala, Sweden).

dx.doi.org/10.1021/ac102895b |*Anal. Chem.* 2011, 83, 2104–2111

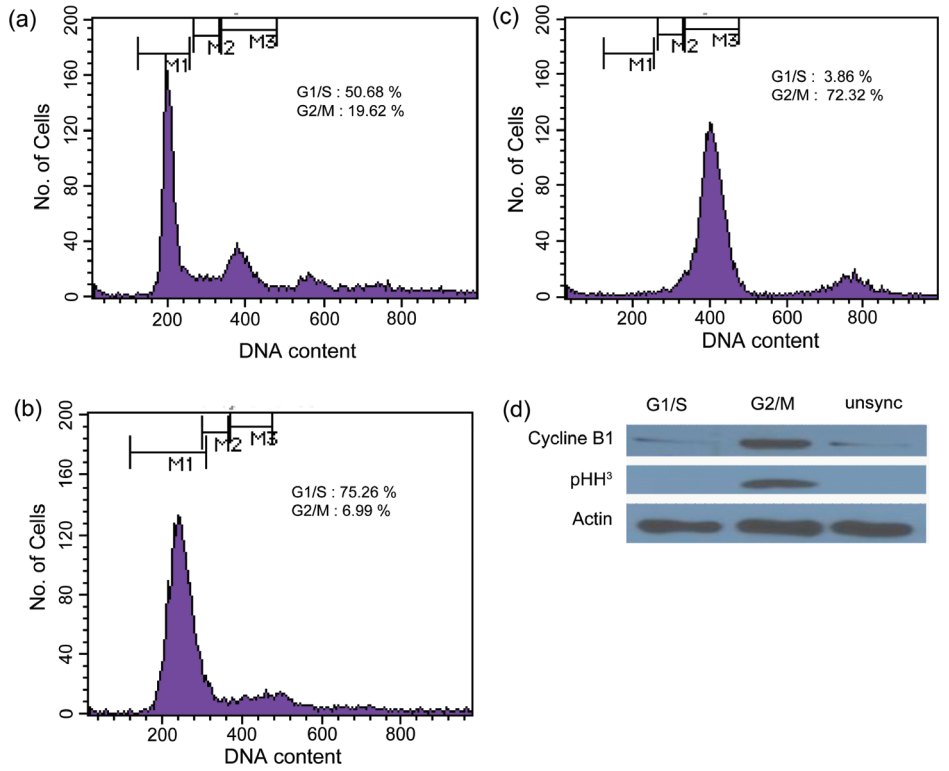

Figure 3. Confirmation of thymidine- and/or nocodazole-mediated cell cycle arrest at the G1/S-phase and G2/M-phase: FACS data show (a) unsynchronized cells in all phases of the cell cycle but mostly G1, (b) cells in the G1/S block, with cells mostly in the G1- and S-phases and decreased in the M-phase, and (c) cells in the G2/M block, with cells mostly in the G2- and M-phases and decreased in other phases. Similarly, (d) a Western blot assay shows expression of p-HH^3 in G2/M-phase cells but not in G1/S-phase or unsynchronized cells, and the highest intensity of cycline B1 was observed in G2/M-phase cells compared to cells in other phases, indicating that most of the cells converted to the G2/M-phase.

RESULTS AND DISCUSSION

Figure 1a illustrates the fabrication process of the cell-attaching electrode (Au/RGD-MAP-C/cell) used for the cell chip. RGD-MAP-C peptide containing a cysteine residue at its terminus was self-assembled on a Au electrode via a Au−S covalent bond, which results in strong attachment of cells to the electrode surface.[14,15] Cell immobilization on a peptide-modified surface leads to establishment of strongly linked integrin receptors on the cell surface.[15,25] The enhanced binding affinities of the cellular receptors to the electrode surface prevent cell detachment caused by washing throughout the experiment, and they also enhance electron transfer during the electrochemical measurements.[16] The unsynchronized cells were then subjected to double thymidine treatment (18 h for each) with an 8 h release by replacing the thymidine-containing media with fresh RPMI 1640, which converted the cells to the G1/S-phase (Figure 1c,i). Similarly, cells in the G2/M-phase were produced by treatment with thymidine for 18 h with a 4 h release, followed by treatment with nocodazole for 10 h as shown in Figure 1c,ii. Consequently, the different electrochemical characteristics of the cells in the G1/S-phase, G2/M-phase, or unsynchronized phase were measured to monitor the intensity or potential difference in voltammetry (arrows indicate DPV signals in Figure 1b).

Electrochemical Characterizations of the Fabricated Cell Chip. The step-by-step surface modification of the Au electrode surface (Figure 1a) was further characterized electrochemically by the DPV method as shown in Figure 2. A strong cathodic peak current appeared (I_{pc}) at +75 mV from the Au/RGD-MAP-C/cell electrode (Figure 2a); however, a very weak peak or no peak was observed from the bare Au or Au/RGD-MAP-C electrode (inset of Figure 2a), which represents the redox reaction of the cells in our system. When the cells immobilized on the Au electrode were exposed to thymidine/thymidine for G1/S-phase block (time scale in Figure 1c,i), a sharp electrochemical signal appeared at +50 mV (Figure 2b), which was different from that of the unsynchronized cells. Remarkably, a new peak was observed at +150 mV during DPV measurement of the cells, which were treated with thymidine/nocodazole for G2/M-phase block (Figure 2b). These differences in DPV signaling from identical cells in different phases (G1/S, G2/M) may have been due to changes in the redox properties of morphologically altered cells.[26] It is well-known that double thymidine treatment blocks the cell cycle in the synthesis phase,[27,28] where DNA replication occurs,[29] and causes remarkable alteration of the cell nucleus.[30] Similarly, thymidine/nocodazole pauses the cell cycle in the M-phase,[28,31,32] where the nucleus becomes divided into two daughter cells.[33] Therefore, the specific DPV signals from cells in the G1/S- and G2/M-phases, which are completely different from unsynchronized cells, can be employed as a tool for the determination of cell cycle arrest.

Confirmation of Cell Synchronization. On-chip synchronization of PC12 cells was confirmed by conventional FACS,[34,35] Western blot analysis using phase-specific proteins (Figure 3), and optical microscopy (Supporting Information, Figure S3). The results show that PC12 cells were successfully

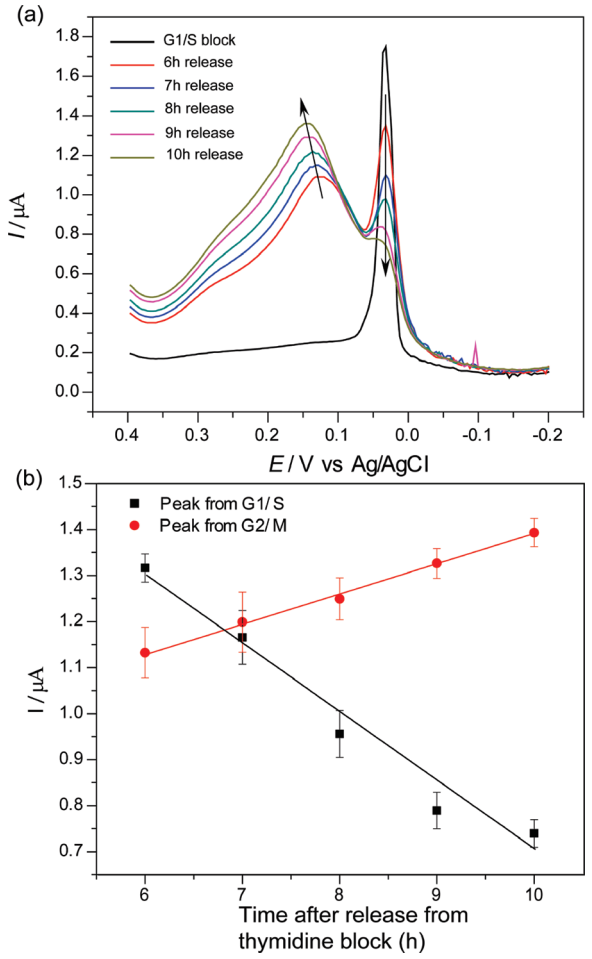

Figure 4. Time-dependent progression of the G1/S-phase toward the G2/M-phase: (a) changes in DPV current peak intensities of PC12 cells after several hours (from 2 to 10 h) of release from G1/S block, where a down arrow indicates a decreased peak from the G1/S-phase and an up arrow indicates an increased peak from the G2/M-phase, (b) a black line indicates a linearly decreased current peak (I_{pc}) from the G1/S-phase in a time-dependent manner (R^2 = 0.99), whereas a red line indicates a linearly increased current peak (I_{pc}) from the G2/M-phase in a time-dependent manner (R^2 = 0.96). Data are the mean ± standard deviation of three different experiments.

synchronized using thymidine and/or nocodazole treatment. Approximately 75% of the cells were fixed in the G1/S-phase (Figure 3b), and 72% were synchronized in the G2/M-phase (Figure 3c), depending on the time of chemical exposure as shown in parts c,i and c,ii, respectively, of Figure 1. These features of synchronized cells were found to differ from those of the unsynchronized group containing a mixture of cells in different phases of the cell cycle (Figure 3a). This indicates successful synchronization of the cells on the chip. On-chip cell synchronization was further confirmed by Western blot analysis using G2/M-phase-specific protein p-HH^3[36−38] and cycline B1.[39−41] Figure 3d shows that p-HH^3 was expressed in the G2/M-phase but absent in unsynchronized and G1/S-blocked cells, whereas cycline B1 was expressed dominantly in G1/S-phase cells.[39,41] These results prove that the cells were successfully synchronized on the chip.

Monitoring of Cell Cycle Progression Based on an Electrochemical Method. After confirmation of cell cycle arrest using conventional methods, the cell chip containing a Au/RGD-MAP-C/cell electrode was employed to measure time-dependent electrochemical characteristics during cell cycle progression. Thymidine-induced G1/S-blocked cells were released for several hours (6, 7, 8, 9, and 10 h) as shown in Figure 1c,iii, and electrochemical measurements were performed at each release time (Figure 4a). The cells in the G1/S-phase produced a sharp peak at a potential of +50 mV, but G2/M-phase cells gave an additional peak at +150 mV that increased with the time of release from double thymidine treatment (Figure 4a). This suggests that G1/S-phase cells progressed to the G2/M-phase as the release period increased. Interestingly, the peak at +50 mV produced by G1/S-phase cells decreased as the new peak increased at +150 mV, which indicates that the new peak was directly related to the number of cells in the G2/M-phase. Moreover, opposite linearity was observed after analysis and quantification of the DPV peak currents measured from the G1/S- and G2/M-phase synchronized chip (Figure 4b). This indicates that G1/S-phase cells gradually progressed to the G2/M-phase as the release period increased. Conversion to the G2/M-phase was observed from 6 h after release, whereas maximum conversion occurred after 10 h of release (Figure 4b). This finding is in agreement with a previous study[6,42] that reported G1/S-phase cells are completely converted to the G2/M-phase after 9−10 h of release from double thymidine block. It is well-known that release from G1/S block allows cells to progress into the M-phase for nuclear division and ultimately cell division.[14] During this phase, cells pass through a number of complex processes, including the prophase, prometaphase, metaphase, anaphase, and telophase, that lead to several changes in the nucleus.[6,43] These cytological changes might be responsible for alterations in the electrochemical behavior of the cell. Therefore, the electrochemical signal is certainly reasonable, on the basis of the observation that the new peak appears as the cell approaches the M-phase and the intensity is increased due to a higher number of cells in the G2/M-phase. Therefore, quantification of the synchronized cells was performed indirectly but accurately by analyzing the current peak obtained from DPV signal intensities using our newly developed electrochemical method.

Validation of Newly Developed Electrochemical Cell Cycle Monitoring. Time-dependent progression of the G2/M-phase was monitored by both conventional FACS[34] and our newly developed electrochemical method. Here, the DPV peak indicating the G2/M-phase appeared when cells were released from G1/S block, and the peak increased upon a longer period of release with a corresponding decrease in the initial peak (Figure 5a, right column), which is in agreement with previous data. Similarly, the histograms obtained from FACS show that the number of cells in the G1/S-phase decreased, which increased the number of cells in the G2/M-phase as the release period increased[28] (Figure 5a, left column). Therefore, DPV peak behavior (Figure 5a, right column) according to time of release from the G1/S-phase was in agreement with the data obtained by the conventional FACS method. Moreover, the trend line derived from analysis and quantification of the peak current (I_{pc}) value increased from the time of release from G1/S block and achieved a maximum at 10 h postrelease (Figure 5b, red line). A similar trend line was also reported by analyzing the numbers of cells that progressed to the G2/M-phase by FACS (Figure 5b, blue line). Therefore, our data obtained

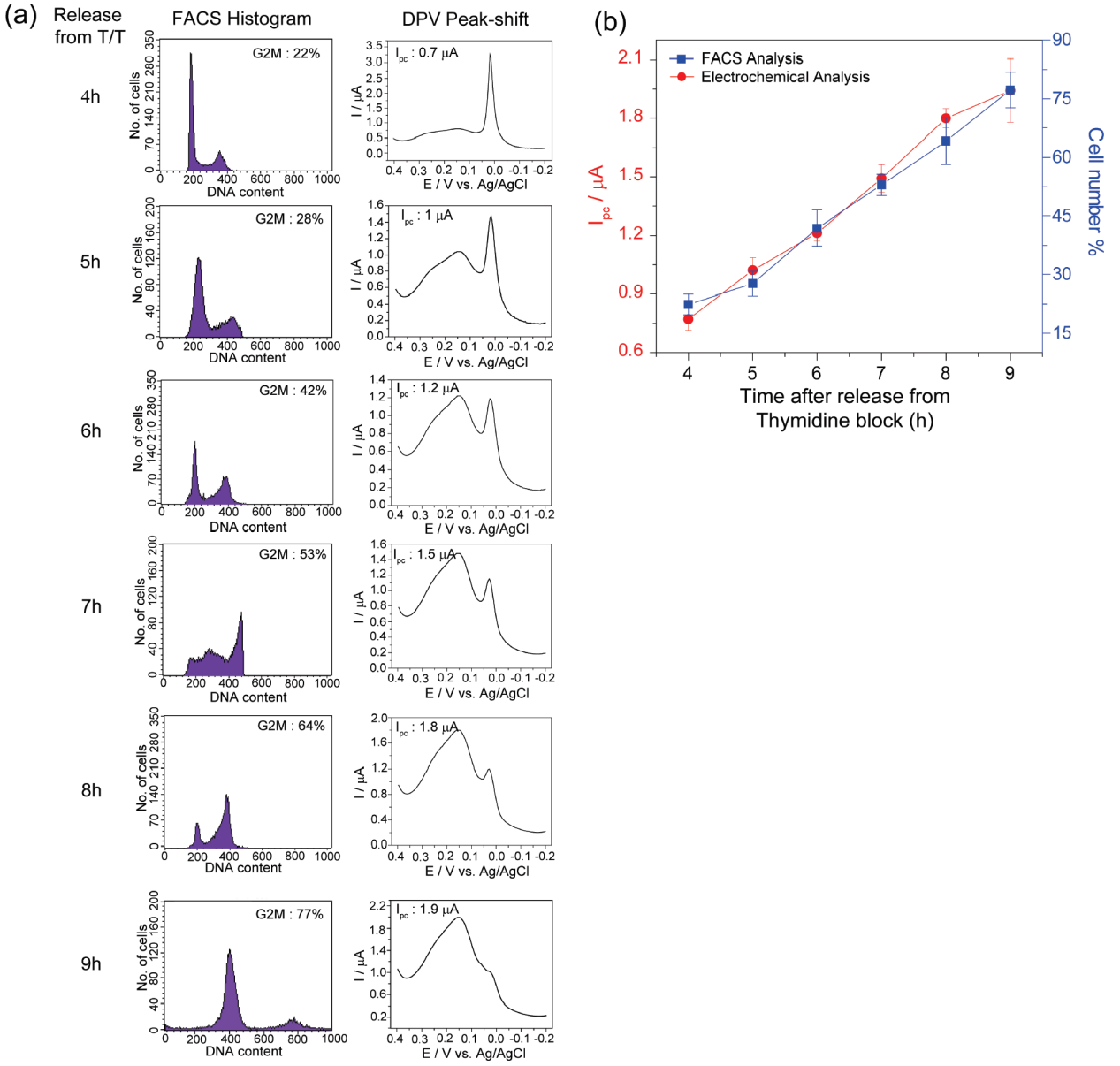

Figure 5. (a) Validation of electrochemical determination of progression of G1/S-phase cells toward the G2/M-phase using FACS (left column) and changes in DPV current peaks (right column) of PC12 cells several hours (from 2 to 10 h) postrelease from G1/S block. (b) Dependence of DPV peak intensities measured from G2/M (red line) and percentage of G2/M-phase cells as measured by FACS (blue line) during the release from double thymidine induced G1/S block. Other conditions were as shown in Figure 2. Data are the mean ± standard deviation of three different experiments.

by the newly developed electrochemical method completely coincided with conventional FACS assay data. Thus, the results of the electrochemical signal using this cell-based electrochemical chip were valid. By using this electrochemical technology, we were able to detect cells in each phase by analyzing and quantifying their DPV signal intensities.

Reproducibility of Electrochemical Cell Cycle Determination Using Varying Numbers of Cells. The number of cells immobilized on each chip was determined to improve the sensitivity of detection as well as to verify reproducibility. For this, varying numbers of cells starting from 0.5×10^5 to 3.5×10^5 cells/mL were allowed to synchronize following the protocol discussed above, and electrochemical measurements were performed accordingly. Figure 6a shows that the current response increased with increasing cell numbers. A concentration-dependent sigmoid curve ($R^2 = 0.99$) was obtained between the current responses and cell numbers (Figure 6b). The concentrations of cells from 1×10^5 to 3×10^5 cells/mL gave exponentially increased signals, whereas decreased signals/nonspecific signals/no signals were observed from the concentrations of cells between 3.5×10^5 and 4.5×10^5 cells/mL (Supporting Information, Figure S4). This phenomenon occurred due to improper synchronization of cells in high density compared to the space of the chip surface.[44] From these results, we found the optimal concentration of cells (3×10^5 cells/mL) for the successful cell synchronization and for achieving maximum signal intensities (Figure 6a). The relative standard deviation of the DPV peak for seven different concentrations of cells ($n = 3$) was 5.6%,

dx.doi.org/10.1021/ac102895b |*Anal. Chem.* 2011, 83, 2104–2111

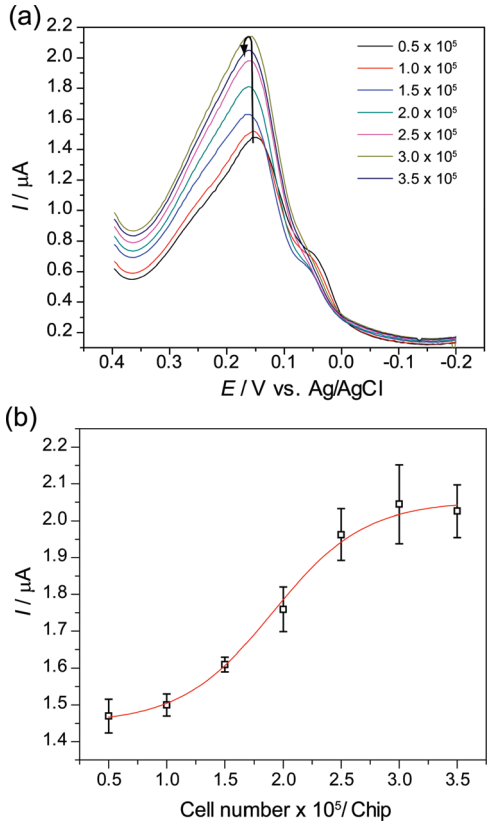

Figure 6. Reproducibility of electrochemical cell cycle determination using varying numbers of cells: (a) Changes in DPV peak intensities corresponding to the various concentrations of PC12 cells on the chip surface (from 0.5×10^5 to 3.5×10^5 cells/mL). An up arrow indicates the increases in peak currents with increasing cell numbers. Cells were synchronized in the G2/M-phase by releasing cells from G1/S block after 10 h for electrochemical recording. (b) A typical sigmoid curve indicates the linear increases in current peaks (I_{pc}) in a concentration-dependent manner ($R^2 = 0.99$). Data are the mean ± standard deviation of three different experiments.x

indicating that the electrochemical cell chip had high sensitivity and reproducibility for cell cycle synchronization.

CONCLUSIONS

We introduced a novel strategy for the detection of cell cycle progression based on cell chip technology. PC12 cells immobilized on the peptide-modified chip surface gave phase-specific redox signals after cell cycle synchronization by thymidine and/or nocodazole treatment. Three kinds of signals were obtained from PC12 cells blocked in the G1/S- and G2/M-phases and unsynchronized cells at potentials of 50, 150, and 75 mV on the basis of the DPV method, respectively. Since the redox signals from the G1/S- and G2/M-phases were clearly differentiated, cell cycle progression in a time-dependent manner could be accurately identified, as well as the number of cells in each phase, which was consistent with the results of conventional FACS and Western blot analysis. Electrochemical determination of the number of cells blocked in the G2/M-phase was also performed to confirm reproducibility. The results show a typical sigmoid curve from current responses corresponding to increases in the concentrations of cells. The origin of the redox signals from cells in each phase, which is the basis of the electrochemical detection method, still needs to be confirmed; however, our research is promising as this new label-free method enables simple, easy, and rapid detection of cell cycle arrest by eliminating the need for fluorescent dyes or antibodies required by conventional analytical techniques. This convenience of our technology offers an advantage for the assessment of the toxicity of common chemicals or efficiency of drugs, since cells in different phases of the cell cycle can have different behaviors even when maintained under the same environmental conditions. Hence, our newly developed method would be useful for the label-free detection of the phase-specific effects of pharmacological compounds and drugs that affect cell growth and division, especially in cancer.

ASSOCIATED CONTENT

Supporting Information. Additional information as noted in the text. This material is available free of charge via the Internet at http://pubs.acs.org.

AUTHOR INFORMATION

Corresponding Author

*Phone: +82-2-705-8480. Fax: +82-2-3273-0331. E-mail: jwchoi@sogang.ac.kr.

ACKNOWLEDGMENT

This work was supported by a National Research Foundation of Korea (NRF) grant funded by the Korean Government (MEST) (2010-0000845), by the Nano/Bio Science & Technology Program (M10536090001-05N3609-00110) of the Ministry of Education, Science, and Technology (MEST), and by the Graduate School of Specialization for Biotechnology Program of the Ministry of Knowledge Economy (MKE).

REFERENCES

(1) Hartwell, L. H.; Weinert, T. A. *Science* **1989**, *246*, 629–634.
(2) Alberts, B.; Johnson, A.; Lewis, J.; Raff, M.; Roberts, K.; Walter, P. *The Molecular Biology of the Cell*; Garland Science, Taylor & Fransis Group: New York, 2002.
(3) Smith, J. A.; Martin, L. *Proc. Natl. Acad. Sci. U.S.A.* **1973**, *70*, 1263–1267.
(4) Nelson, D. M.; Ye, X.; Hall, C.; Santos, H.; Ma, T.; Kao, G. D.; Yen, T. J.; Harper, J. W.; Adams, P. D. *Mol. Cell. Biol.* **2002**, *22*, 7459–7472.
(5) Nyberg, K. A.; Michelson, R. J.; Putnam, C. W.; Weinert, T. A. *Annu. Rev. Genet.* **2002**, *36*, 617–656.
(6) Cude, K.; Wang, Y.; Choi, H. J.; Hsuan, S. L.; Zhang, H.; Wang, C. Y.; Xia, Z. *J. Cell Biol.* **2007**, *177*, 253–264.
(7) Li, F.; Ambrosini, G.; Chu, E. Y.; Plescia, J.; Tognin, S.; Marchisio, P. C.; Altieri, D. C. *Nature* **1998**, *396*, 580–584.
(8) Leung, B. S.; Potter, A. H. *J. Cell. Biochem.* **1987**, *34*, 213–225.
(9) Bowen, W. P.; Wylie, P. G. *Assay Drug Dev. Technol.* **2006**, *4*, 209–221.
(10) Samaké, S.; Smith, L. C. *Theriogenology* **1997**, *48*, 969–976.
(11) Xiang, Y.; Cox, H.; Lebedeva, I.; Coleman, J.; Shen, D.; Pande, P.; Schultz, J.; Patton., W. F. *Nat. Methods* **2009**, *6*, an2–an3.
(12) Wong, J. T. Y.; Whiteley, A. *J. Exp. Mar. Biol. Ecol.* **1996**, *197*, 91–99.
(13) Nunez, R. *Mol. Biol.* **2001**, *3*, 67–70.
(14) Jin, H. S.; Lee, T. H. *Biochem. J.* **2006**, *399*, 335–342.
(15) Kafi, M. A.; Kim, T.-H.; Yea, C.-H.; Kim, H.; Choi, J.-W. *Biosens. Bioelectron.* **2010**, *26*, 1359–1365.
(16) Kafi, M. A.; Kim, T.-H.; Yagati, A. K.; Kim, H.; Choi, J.-W. *Biotechnol. Lett.* **2010**, *32*, 1797–1802.

(17) El-Said, W. A.; Yea, C.; Kim, H.; Oh, B. K.; Choi, J.-W. *Biosens. Bioelectron.* **2009**, *24*, 1259–1265.
(18) El-Said, W. A.; Yea, C.-H.; Kwon, I.-K.; Choi, J.-W. *Biochip J.* **2009**, *3*, 105–112.
(19) Choi, J. W.; Nam, Y. S.; Fujihira, M. *Biotechnol. Bioprocess Eng.* **2004**, *9*, 76–85.
(20) May, K. M.; Wang, Y.; Bachas, L. G.; Anderson, K. W. *Anal. Chem.* **2004**, *76*, 4156.
(21) Yea, C. H.; Min, J.; Choi, J. W. *Biochip J.* **2007**, *1*, 219–227.
(22) Wang, L.; Wang, L.; Yin, H.; Xing, W.; Yu, Z.; Guo, M.; Cheng, J. *Biosens. Bioelectron.* **2010**, *25*, 990–995.
(23) Gutierrez, G. J.; Tsuj, T.; Cross, J. V.; Davis, R. J.; Templeton, D. J.; Jiang, W.; Ronai, Z. A. *J. Biol. Chem.* **2010**, *285*, 14217–14228.
(24) Zhu, H.; Boobis, A. R.; Gooderham, N. J. *Cancer Res.* **2000**, *60*, 1283–1289.
(25) Ruoslahti, E. *Annu. Rev. Cell Dev. Biol.* **1996**, *12*, 697–715.
(26) Mitchison, T. J.; Salmon, E. D. *Nat. Cell Biol.* **2001**, *3*, E17–E21.
(27) Huberman, J. A. *Cell* **1981**, *23*, 647–648.
(28) Zhu, H.; Nigel, J. *Toxicol. Sci.* **2006**, *91*, 132–139.
(29) McCulloch, S. D.; Kunkel, T. A. *Cell Res.* **2008**, *18*, 148–161.
(30) Lengronne, A.; Pasero, P.; Bensimon, A.; Schwob, E. *Nucleic Acids Res.* **2001**, *29*, 1433–1442.
(31) Krek, W.; DeCaprio, J. A. *Methods Enzymol.* **1995**, *254*, 114–124.
(32) Zieve, G. W.; Turnbull, D.; Mullins, J. M.; McIntosh, J. R. *Exp. Cell Res.* **1980**, *126*, 397–405.
(33) Reddy, G. P. *J. Cell. Biochem.* **1994**, *54*, 379–386.
(34) Resnitzky, D.; Gossen, M.; Bujard, H.; Reed, S. I. *Mol. Cell. Biol.* **1994**, *14*, 1669–1679.
(35) Futcher, B. *Methods Cell Sci.* **1999**, *21*, 79–86.
(36) Kaitna, S.; Pasierbek, P.; Jantsch, M.; Loidl, J.; Glotzer, M. *Curr. Biol.* **2002**, *12*, 798–812.
(37) Cortez, D.; Guntuku, S.; Qin, J.; Elledge, S. J. *Science* **2001**, *294*, 1713–1716.
(38) Crosio, C.; Fimia, G. M.; Loury, R.; Kimura, M.; Okano, Y.; Zhou, H.; Sen, S.; Allis, C. D.; Sassone-Corsi, P. *Mol. Cell. Biol.* **2002**, *22*, 874–885.
(39) Cogswell, J. P.; Godlevski, M. M.; Bonham, M.; Bisi, J.; Babiss, L. *Mol. Cell. Biol.* **1995**, *15*, 2782–2790.
(40) Norbury, C.; Nurse, P. *Annu. Rev. Biochem.* **1992**, *61*, 441–470.
(41) Pines, J.; Hunter, T. *Cell* **1989**, *58*, 833–846.
(42) Langan, T. J.; Slater, M. C.; Kelly, K. *Glia* **1994**, *10*, 30–39.
(43) Huang, J. N.; Park, I.; Ellingson, E.; Littlepage, L. E.; Pellman, D. *J. Cell Biol.* **2001**, *154*, 85–94.
(44) Bartholomew, J. C.; Neff, N. T.; Ross, P. A. *J. Cell Physiol.* **1976**, *89*, 251–258.